Proceedings of 1st Croatian Conference on Earthquake Engineering, 1CroCEE
Zagreb, Croatia - March 22nd to 24nd, 2021
Edited by Laksusic, S. and Atalic, J.
Copyright © 2021 CroCEE

Component Tests, Fracture Simulation, and Experimental Study on Steel Damper for passive energy dissipation

Ferit Gashi[(1)], Francesco Petrini[(2)], Franco Bontempi[(3)]

[(3)] Professor, Department of Structural and Geotechnical Engineering, Sapienza University of Rome
E-mail: Franco.Bontempi@Uniroma1.it

[(2)] Assistant Professor, Department of Structural and Geotechnical Engineering, Sapienza University of Rome
E-mail: Francesco.petrini@Uniroma1.it

[(1)] Department of Structural and Geotechnical Engineering, Sapienza University of Rome
E-mail: Gashi.1670547@studenti.uniroma1.it, Ferittgashi@gmail.com

Abstract

This paper summarizes the experimental campaign carried out for the development of a new steel energy dissipative device named Slit Dampers (SDs) designed for earthquake protection of structures. SDs consist in shear steel plates with appropriately shaped cut-out portions of material for allowing the maximum spread of plastic deformation along the device and then maximizing the hysteretic dissipative behavior. A total of eighty-two steel shear plates with different openings and thicknesses are tested to investigate their behavior under cyclic pseudo-static loading. Six types of steel shear plates are studied, including the SD with narrow slits that divide the plate into rectangular links, and the butterfly fuse with a diamond-shaped opening that creates butterfly shape links in the plate. Other varying test parameters are loading rate, material strength, and the number of in-parallel damper elements. It is expected that the proposed model can be successfully used to predict the behavior of dampers in real-world applications.

Keywords: Experimental, Energy dissipation, Cyclic load, Metalic damper, Hysteresis Model, etc.

1.0 INTRODUCTION

Conventional design concepts of earthquake-resistant structures are not intended to avoid damage on the structures but to ensure the safety of humans under severe earthquakes. Dampers are passive control systems or passive energy dissipation devices that are implemented in the structures to protect against seismic excitation. Passive control systems absorb energy induced by an earthquake in various mechanisms, such as metal yielding, friction, fluid orifice, and viscous elastic deformation of solid. These passive control systems are categorized based on their dispersing mechanisms: metallic ADAS-device [3] , Tadas-device [2], friction, thick liquid , and viscoelastic dampers (rigid) [19]. Metal dampers dissipate energy through inelastic deformation and provide a stable hysterical envelope. Excellent hysteretic behavior, easy accessibility, simple replacement after an earthquake, and low fabrication costs are some advantages of steel slit dampers [6]. Slit devices can be used at different configurations such as bracing joints [2,4,6], beam-to-column connections [18], and steel slit walls as fuses [18,6,3]
This paper concentrates on a detailed investigation of the structural performance of a slit damper and butterfly damper proposed by the authors. With this purpose in mind, various conditions focusing on real-world applications of the damper were established as variables, specifically loading type, loading rate mm/s, the material strength of the steel, and the number of damper plates used. From the experimental results, the structural characteristics are compared and discussed in terms of failure mode, strength, stiffness, deformation, and energy dissipation.

Copyright © 2021 CroCEE

2.0 Device design

The Dampers were manufactured in Kosovo, using water cutting technology(Fig.1, Fig.2). Water cutting capabilities were found to be common in large machine shops and therefore not expensive. The slits are rounded at their ends, thereby reducing stress concentration in reentrant-corners. The device is a weld-free design, thus eliminating the uncertainties and imperfections associated with welding.

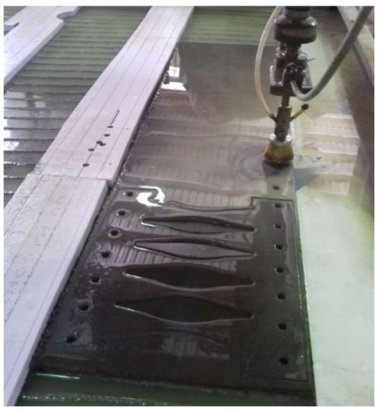

Fig.1.Shows the water cutting process

Fig.2 After water cutting

Elastic moment of bending in the slit, Under sufficient displacement, plastic hinges are formed at both ends of each strip. Consequently, the mechanical properties of the crack absorber can be described in relation to the length of the strip L0, strip depth b, and thickness t(Fig.3). Supposing elastic behavior perfect plastic, the device gives the load **P**y can be determined based on an analysis of the plastic mechanism.

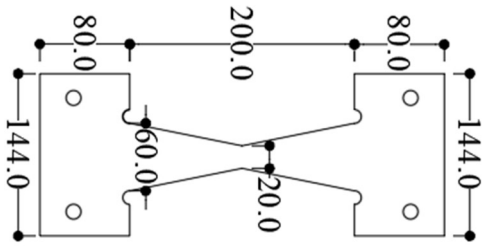

Fig.3 Details of the test specimens

Specimens	Material	Thickness	Width (mm)	Height (mm)	Loading Amp
Specimens.A1	S-235	20	60	200	Constant-A1
Specimens.A2	S-235	20	60	200	Constant-A2
Specimens.A3	S-235	20	60	200	Constant-A3
Specimens.A4	S-235	20	60	200	Constant-A4
Specimens.B1	S-235	3	60	200	Increasing-AISC
Specimens.B2	S-275	10	60	200	Increasing-AISC
Specimens.B3	S-235	20	60	200	Increasing-AISC

Table 1:Table test specimens

Proceedings of 1st Croatian Conference on Earthquake Engineering, 1CroCEE
Zagreb, Croatia - March 22nd to 24nd, 2021
Edited by Laksusic, S. and Atalic, J.
Copyright © 2021 CroCEE

3.0 Experimental Program

3.1 Test Specimens

The specimen properties are listed in *Table 1*.

3.2 Loading Protocol

Cyclic tests were carried out on 4 specimens:
Constant cyclic loading, in which maximum displacement (Dmax) is constant over the entire cycle as 15 mm (Specimen A1), 35 mm (Specimen A2), 48 mm (Specimen A3), and 56 mm (Specimen A4). The purpose of this program is to obtain fatigue parameters.
The loading protocol for the steel damper test was created based on the AISC code loading. The AISC protocol was modified by adding three extra sets of six low amplitude cycles preceding the prescribed loading procedure.

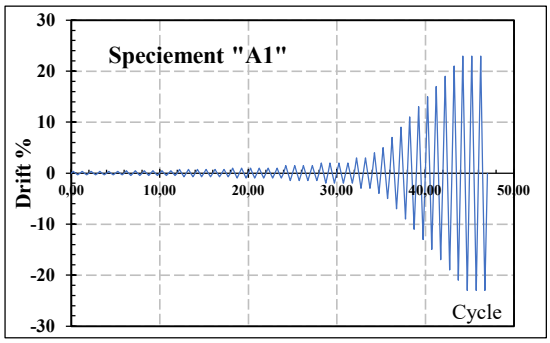

Fig.4 -AISC Modified protocol

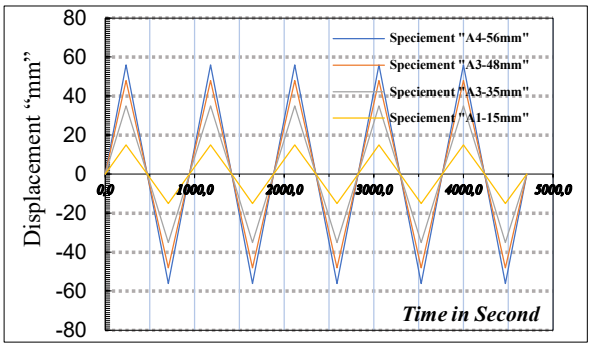

Fig.5-Constat cyclic

3.3 Experiment Setup

Various types of cyclic tests were performed using a 500 kN hydraulic servo fatigue test machine MTS Loading was controlled by displacement with an inner displacement transducer mounted on the test machine. The loading rate (v) was fixed as 0.5 mm/s, except for incremental amplitude cycling.Fig.6

3.4 Material Properties

Plate Material Tests, five dogbone-shaped tension coupon tests were conducted on the fuse plate material. the tests took place at the Department of Structural and Geotechnical Engineering. the coupon specimens were tested using an MTS machine in fig.7


(a) (b)
Fig.7 Coupon test setup: a)Before the test, b)Necking

Copyright © 2021 CroCEE

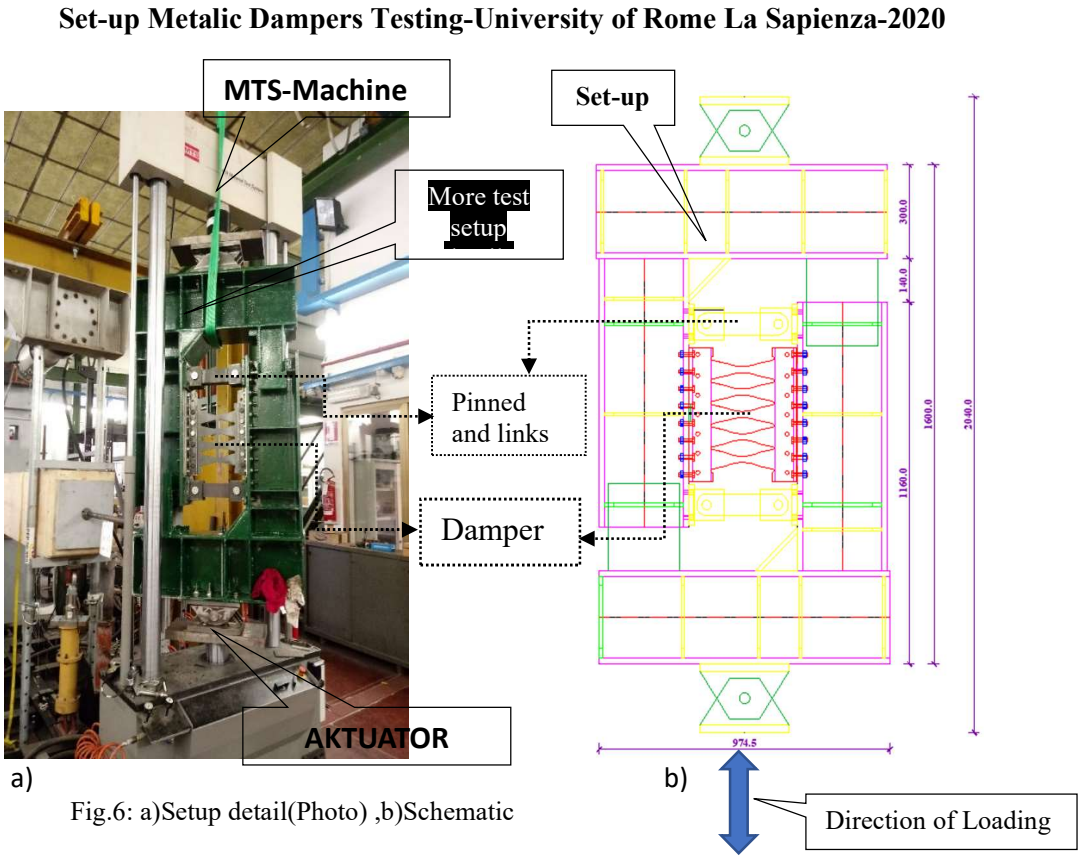

Fig.6: a)Setup detail(Photo) ,b)Schematic

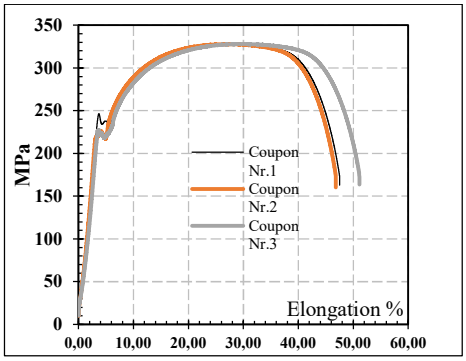

Fig.8- Engineering stress-strain curves S-235

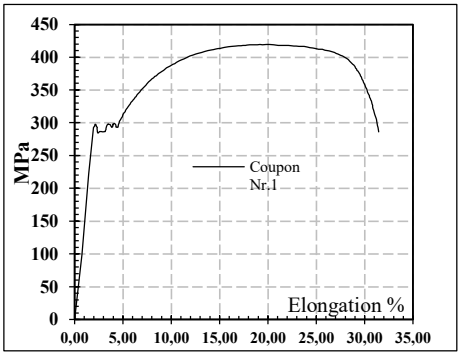

Fig.8"- engineering stress-strain curves S-275

Three types of steel were selected: S-235, S-275. Fig.8 demonstrates their constitutive curves obtained through uniaxial tensile tests and *table 2.*

Coupon S-235	Fy (MPa)	Fu (MPa)	Elongation %	E	Coupon S-275	Fy (MPa)	Fu(MPa)	Elongation %	E
1	246,3	327,3	45,2	200 000	1	291,3	425,3	37,5	200 000
2	219,0	328,0	50,0	200 000	2	295,3	426,1	40,4	200 000
3	227,1	328,0	49,6	200 000					
Average	**230.8**	**327.8**	**48.3**	**200 000**	**Average**	**293.3**	**425.7**	**38.95**	**200 000**

Table 2 - Summary of mechanical properties

Copyright © 2021 CroCEE

4.0 TEST RESULTS

Four specimens deformed stably under the cyclic tests. Specimens butterfly was loaded until fracture during the tests. Ductile cracks initiated at the toe of the butterfly close to the rounded toes of the slits during the loading of all specimens. Under further loading, those cracks propagated wider and longer, which led to the decrease of the load-carrying capacity of the dampers.
It is clear that all specimens have yielded at large displacement and exhibited very stable hysteric behavior and the shape of the loops which close to a rectangular indicates high energy dissipation capacity. Strength degradation started to appear when cracks slowly formed at the ends of the rounded corner of fixed ends due to stress concentration, which propagated longer and wider during the test until the specimen reached fracture. The tests were stopped after steel plates completely fractured and the load sustained was significantly reduced.

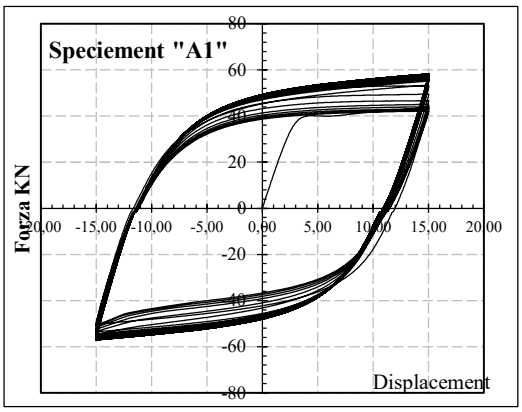

Fig.9 . Force-displacement hysteresis(SpeciementA1-15mm)

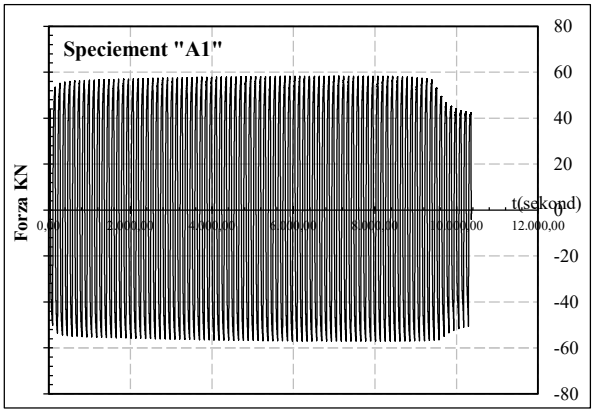

Fig.10 . Time History, Force-time(s)

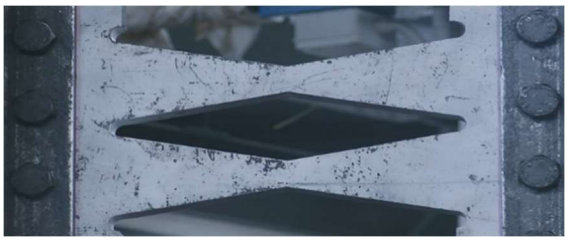

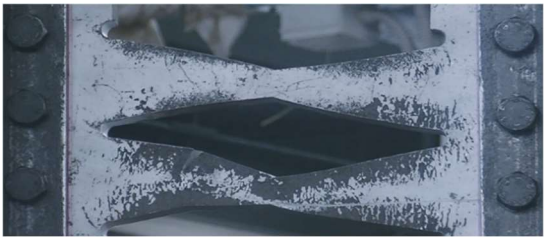

a) b)

Fig.11 . Photo of Speciements A1: aStart of the test,b) Fracture-end test

Link: https://www.youtube.com/watch?v=oG46PPyLIrw&t=260s

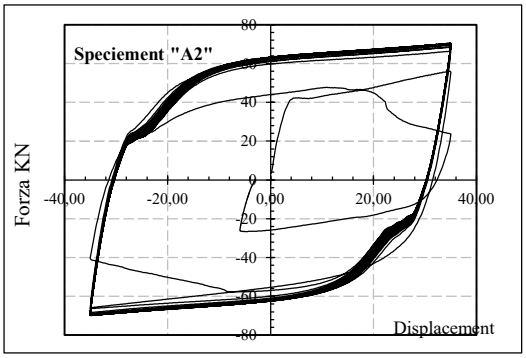

Fig.12 . Force-displacement hysteresis(SpeciementA2-35mm)

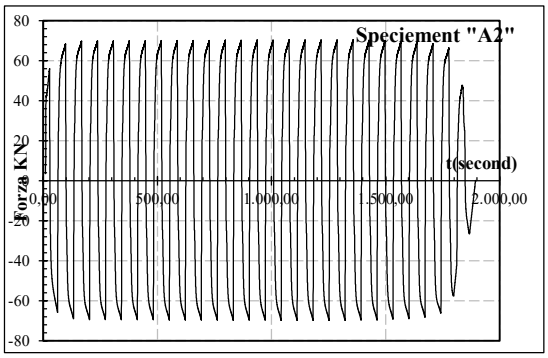

Fig.13 . Time History(SpeciementA2), Force-time(s)

Proceedings of 1st Croatian Conference on Earthquake Engineering, 1CroCEE
Zagreb, Croatia - March 22nd to 24nd, 2021
Edited by Laksusic, S. and Atalic, J.
Copyright © 2021 CroCEE

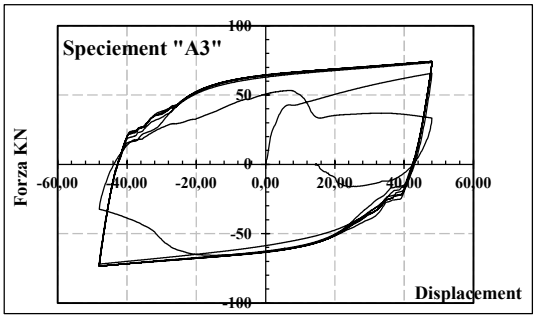

Fig.14 .Force-displacement hysteresis(SpecimA3-48mm)

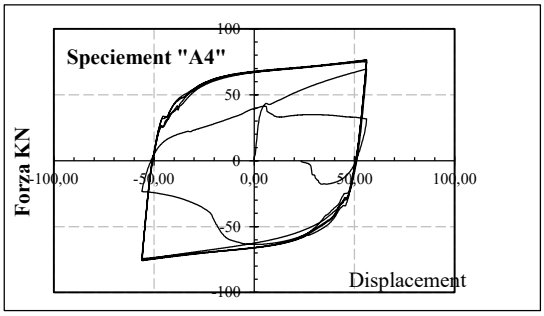

Fig.15 Force-displacement hysteresis(SpeciemA3-56mm)

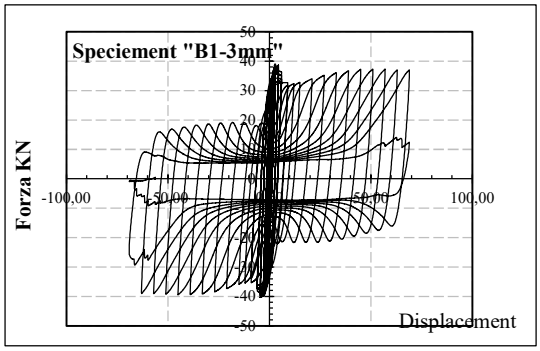

Fig.16 . Force-displacement hysteresis(SpeciemB1-3mm)

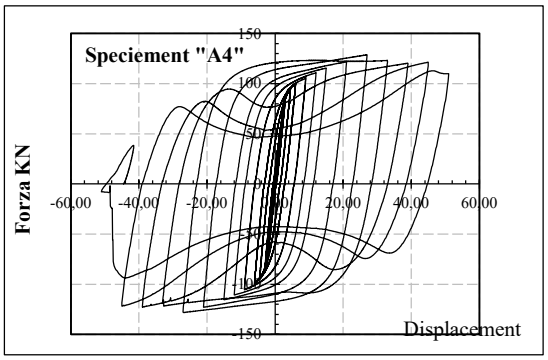

Fig.17. Force-displacement hysteresis(SpeciemB2-8mm)

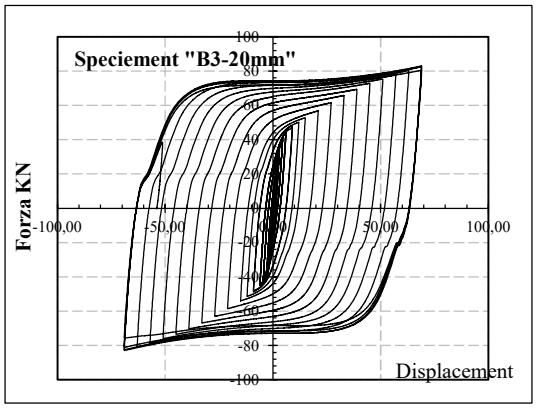

Fig.18 Force-displacement hysteresis(SpeciementB2-8mm)

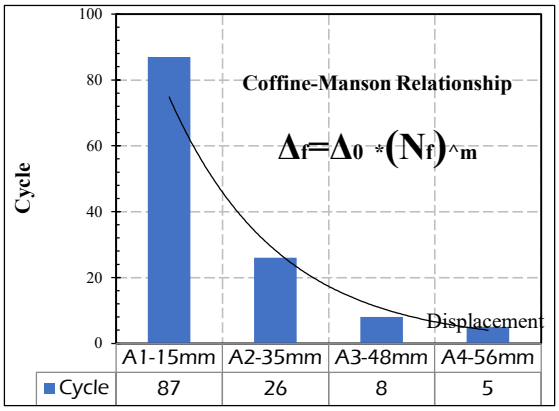

Fig.19 . Low Cycle Coffine-Manson.

5.0 Energy dissipation

To investigate the effect of test parameters on the energy dissipation capacity of dampers, hysteretic curves for dissipated energy were shown in *Fig.16,Fig.17, Fig.18*. The dissipated energy of specimens with depth ratio (B/t) of 66.67, 25, and 10 is higher than that of specimens with depth ratio of 3mm,8mm, 20mm.

Specimens B1 with a depth 3mm, which have steel plates with the least depth variation, dissipated energy very low and failed at a relatively low cumulative displacement,*Fig.16*.

Specimens B2 with a depth of 8mm, which have steel plates with the least depth medium, dissipated energy very large and failed at a relatively medium cumulative displacement*Fig.17.*

Specimens B3 with a depth of 20mm, which have steel plates with the depth large, dissipated energy very large and failed at a relatively large cumulative displacement,*Fig.18*.

Figure 9 shows the failure mode of the A1 specimen under constant cyclic loading. For A1, small

Proceedings of 1st Croatian Conference on Earthquake Engineering, 1CroCEE
Zagreb, Croatia - March 22nd to 24nd, 2021
Edited by Laksusic, S. and Atalic, J.
Copyright © 2021 CroCEE

cracks start to occur at the 78th repeated cycle. After repeatedly receiving more than 63 tensile and compressive loads, the cracks gradually deepened at the expected plastic hinge location and finally fractured with a sudden load reduction beyond the 82nd cycle, marking the end of the experiment. The low-cycle fatigue test of the coke damper indicates that the coke damper exhibits resistance to low-cycle fatigue with sufficient inelastic deformation beyond the 82th cycle after yielding, and the final fracture occurs at the expected plastic locations,*Fig.9*.
Figure 12 shows the failure mode of the A2 specimen under constant cyclic loading. For A2, small cracks start to occur at the 24th repeated cycle. After repeatedly receiving more than 28 tensile and compressive loads, the cracks gradually deepened at the expected plastic hinge location and finally fractured with a sudden load reduction beyond the 32nd cycle, marking the end of the experiment. The low-cycle fatigue test of the coke damper indicates that the coke damper exhibits resistance to low-cycle fatigue with sufficient inelastic deformation beyond the 32th cycle after yielding, and the final fracture occurs at the expected plastic locations.
Figure 14 shows the failure mode of the A3 specimen under constant cyclic loading. For A3, small cracks start to occur at the 6th repeated cycle. After repeatedly receiving more than 6 tensile and compressive loads, the cracks gradually deepened at the expected plastic hinge location and finally fractured with a sudden load reduction beyond the 8nd cycle, marking the end of the experiment. The low-cycle fatigue test of the coke damper indicates that the coke damper exhibits resistance to low-cycle fatigue with sufficient inelastic deformation beyond the 8th cycle after yielding, and the final fracture occurs at the expected plastic locations.
Figure 15 shows the failure mode of the A4 specimen under constant cyclic loading. For A4, small cracks start to occur at the 4th repeated cycle. After repeatedly receiving more than 4 tensile and compressive loads, the cracks gradually deepened at the expected plastic hinge location and finally fractured with a sudden load reduction beyond the 5nd cycle, marking the end of the experiment. The low-cycle fatigue test of the coke damper indicates that the coke damper exhibits resistance to low-cycle fatigue with sufficient inelastic deformation beyond the 5th cycle after yielding, and the final fracture occurs at the expected plastic locations.

6. Conclusions

The present paper presents the experimental study of steel slit-dampers with various depth.The number of loading cycles until the ultimate state of a slit-damper is found to match very well to the Manson-Coffin relation *Fig.19*.
The following conclusions are made from this study:
1. Damper configuration with increased height of the strip has low stiffness and provides stable hysteretic curve under large displacement irrespective of strip width at mid-height.
2. Reducing the strip width at the mid-height has a high influence on the damper performance by avoiding brittle damage at the end from stress concentration.
3. Further, varying the thickness and strip width at mid-height enhance the damping of the specimen.
4. Based on the response surface methodology, effective stiffness and effective damping is expressed as a function of strip width at mid-height (bc), height of the strip (h) and thickness of the damper (t).

Acknowledgements

The authors would like to thank prof.Dr.Franco Bontempi from the "La Sapienza" University of Rome. In addition, the authors wish to acknowledgements the technical staff at the Structural Testing Laboratory at the Sapienza University of Rome.

Proceedings of 1st Croatian Conference on Earthquake Engineering, 1CroCEE
Zagreb, Croatia - March 22nd to 24nd, 2021
Edited by Laksusic, S. and Atalic, J.
Copyright © 2021 CroCEE

References

[1] Abaqus(2014).Abaqus analysis user's manual, version 16.4
[2] Aiken,I.,Nims,d.Whittaker,A.,and Kelly,J.(1993). "Testing of passive energy dissipation systems"
[3] Kobori,T.,Miura,Y.Fukusawa,E Yamada,T.,Arita,T..,and Takenake,Y(1992) "Development and application of hysteresis steel dampers" Proc.11th World Conference on Earthquake Engineering.
[4] Amadeo B.,Sang-Hoon OH.,Akiyama.H.(1998) "Ultimate energy absorption capacity of slit type steel plates sbjected to shear deformations
[5] ASCE. (2010). "Minimum design loads for buildings and other structures." ASCE/SEI 7-10, ASCE, Reston, VA.
[6] Chan, R. W. K., and Albermani, F. (2008). "Experimental study of steel slit damper for passive energy dissipation." Eng. Struct., 30(4), 1058–1066.
[7] Dowling, N. E. (2007). Mechanical behavior of material: Engineering methods for deformation, fracture, and fatigue, 3rd Ed., Prentice Hall, NJ.
[8] Fatemi, A., and Vang, L. (1998). "Cumulative fatigue damage and life prediction theories: A survey of the state of the art for homogeneous materials." Int. J. Fatigue, 20(1), 9–34.
[9] FEMA. (2000). "Prestandard and commentary for the seismic rehabilitation of buildings." Rep. No. FEMA-356, FEMA, Washington, DC.
[10] FEMA. (2007). "Interim testing protocol for determining the seismic per-formance characteristics of structural and nonstructural components." Rep. No. FEMA-461, FEMA, Washington, DC.
[11] Ju, Y. K., Kim, M. H., Kim, J., and Kim, S. D. (2009). "Component tests of buckling-restrained braces with unconstrained length." Eng. Struct., 31(2), 507–516.
[12] Kim, Y. J., Jung, I. Y., Ju, Y. K., Park, S. J., and Kim, S. D. (2010). "Cyclic behavior of diagrid nodes with H-section braces." J. Struct. Eng., 136(9), 1111–1122.
[13] Krawinkler, H., and Zohrei, M. (1983). "Cumulative damage in steel structures subjected to earthquake ground motions." Comput. Struct., 16(1–4), 531–541.
[14] Miner, M. A. (1945). "Cumulative damage in fatigue." J. Appl. Mech., 12(3), 159–164
[15] Mackenzie, A. C., Hancock, J.W. & Brown, D. K. (1977), 'On the influence of state of stress on ductile failure initiation in high strength steels', Engineering Fracture Mechanics **9**(1), 167–188.
[16] Kanvinde, A. M. & Deierlein, G. G. (2006), 'The void growth model and the stress modified critical strain model to predict ductile fracture in structural steels', Journal of Structural Engineering **132**(12), 1907–1918
[17] Skinner, R. I., Kelly, J. M. & Heine, A. J. (1975), 'Hysteretic dampers for earthquake-resistant structures', Earthquake Engineering & Structural Dynamics
[18] Oh, S. H., Kim, Y.-J., and Ryu, H.-S. (2009). "Seismic performance of steel structures with slit dampers." Eng. Struct.
[19] Christopoulos C, Montgomery M. Viscoelastic coupling dampers (VCDs) for enhanced wind and seismic performance of high-rise buildings. Earthq Eng Struct Dyn 2013
[20] Chopra, A. K. (2019): *Dynamic of structures*. Pearson Education, 5th edition, United States.
[21] Bruneau M., Uang C.M. and Sabelli R., *Ductile design of steel structures,* McGraw Hill, Inc, 2011.